

A compact multi-band notched characteristics UWB microstrip patch antenna with a single sheet of graphene

Noor Raheem, Nidal Qasem

Department of Electronics and Communications Engineering, Faculty of Engineering,
Al-Ahliyya Amman University, Jordan

Article Info

Article history:

Received Oct 10, 2019

Revised Jan 6, 2020

Accepted Mar 2, 2020

Keywords:

Graphene

Microstrip patch antenna

Notch-characteristics

Reconfigurability

Ultra wideband antenna

ABSTRACT

A rectangular tuneable ultra-wideband (UWB) microstrip patch (MP) antenna based on a single sheet of graphene (SSG) is designed in this study. The antenna band can be tuned by applying a DC voltage bias perpendicular to the SSG at various values via adjusting the input impedance. The antenna has been analyzed by computer simulation technology (CST) microwave studio (MWS) software using an FR4 substrate of thickness 1.6 mm with a dielectric permittivity $\epsilon_r = 4.4$ and loss tangent $\tan \delta = 0.02$ fed by a 50Ω microstrip line frequency. The design is compact since the antenna consists mostly of copper and the SSG. Graphene's low weight, high flexibility, and strength make it more attractive than other semiconductor materials. Then, the study investigates the effects of applying the electrical characteristics of graphene to the antenna's length, which varies with the ON and OFF states. This UWB MP antenna is also designed with notch characteristics so that it can reject undesired interference signals. Subsequently, this compact UWB MP antenna with tuneable resonance frequency is suitable for most wireless communication applications. The simulation results work in the 3.1 to 10 GHz range, as required for UWB technology.

This is an open access article under the [CC BY-SA](https://creativecommons.org/licenses/by-sa/4.0/) license.



Corresponding Author:

Nidal Qasem,

Department of Electronics and Communications Engineering, Faculty of Engineering,

Al-Ahliyya Amman University,

Zip-code (Postal Address): 19328, Amman, Jordan.

Email: Ne.qasem@ammanu.edu.jo

1. INTRODUCTION

Ultra-wideband (UWB) technology is attractive for wireless applications of promising communications methods. In the USA, the Federal Communications Commission (FCC) restricts the UWB frequency spectrum between 3.1 to 10.6 GHz range. UWB antennas are desired for different applications such as wireless communications, military purposes, indoor positioning, and medical applications due to their ability to transmit a very high bit rate with a low power spectrum [1, 2].

Microstrip patch (MP) antennas are used most frequently in UWB antenna designs due to advantages such as being light-weight, compactable, inexpensive, and compact. Moreover, MP antennas have a wide operating bandwidth and exhibit omnidirectional patterns [3]. With such wide applications across the spectrum, an absorbing material is required to absorb waves with changes in the resonant frequency. One such absorbing material is a graphene impedance surface, which enhances the performances of various antennas by changing their resonance frequencies via the implementation of an external DC voltage

bias. Hence, changing the impedance values leads to the mimicry of the ON and OFF states found in switches [4, 5].

Graphene is a two-dimensional atomic material that consists of carbon atoms organized in a hexagonal lattice. In addition, graphene has special characteristics that make it an attractive material for smart devices. In particular, the absorption of an unbiased original single sheet of graphene (SSG) is exactly 2.3% of incoming light. Graphene, has been widely investigated for in optical, thermal, medical, electronic, and more other applications [5, 6]. The literature presents different designs for antennas such as antenna having square slot [7], a loaded pad of graphene on an MP antenna [8], different UWB designs [9], a graphene based conductor for a UWB antenna [10], a novel transparent UWB antenna [11], an MP antenna with enhanced gain and bandwidth for UWB wireless applications [2], and interference mitigation using slot cutting in UWB antenna [12].

Antenna size is an important factor in controlling operational bandwidth, where increasing the dimensions of the antenna will increase the operational band range. To achieve a small size for an UWB antenna, the antenna proposed in this study has a new configurable design based on graphene material [5]. The graphene be tuned by implementing an associated electric field perpendicular to the graphene layer, which will change the physical length of the structure in the ON and OFF states. Therefore, the antenna match and tuneable frequency band will be enhanced. The resulting UWB antenna has a high bit rate and low power consumption, thus is increased [13].

This paper will introduce a description about the probability of minimizing the size of the UWB antenna and increase in the operational bandwidth with additional tunable band-notched antenna. This can be done by configuring the design based on graphene material operates with UWB. This paper is arranged as follows: section 2 explains the proposed antenna design, how to implement the graphene material, and the performance of UWB MP antenna with SSG using computer simulation technology (CST) microwave studio (MWS) [14]. Next, section 3 discusses the simulation results. Finally, the conclusion is summarized in section 4.

2. PROPOSED ANTENNAS DESIGN

2.1. MP antenna

An MP antenna is small, low weight, and easy to fabricate; these characteristics and more meet the needs of wireless communication applications. Figure 1 displays the front and back views of the proposed antenna. The antenna is designed on an FR4 substrate with a thickness of 1.6 mm with dielectric relative permittivity $\epsilon_r = 4.4$ and loss tangent $\tan \delta = 0.02$ fed by a 50 Ω microstrip line frequency where the ground plane is on the other side of the substrate. A microstrip feed line technique is used for feeding the antenna due to its ease of fabrication and easy matching. The patch is rectangular and the total size of the proposed antenna including the substrate is 23.9x28.5 mm. The patch dimensions are $W_p \times L_p$, and it consists of two rectangular steps—one larger than the other with dimensions $L_1 \times W_1$ and $L_2 \times W_2$. The feed line's width and length are denoted by (W_f) and (L_f), respectively, the ground plane's high is represented by (L_g), and there is a gap (G) between the patch and ground plane. There is also a slot cut out of the ground plane with dimensions $L_{slot} \times W_{slot}$ which has been included to enhance the impedance matching at the higher frequency band more than the lower band.

For this proposed design of UWB antenna with a rectangular MP, the essential parameters are set as: frequency of operation (f_o) = 7.5 GHz, dielectric constant of the substrate (ϵ_r) = 4.4, and height of dielectric substrate (h) = 1.6 mm [15, 16]:

$$W_p = \frac{c}{2f_o \sqrt{\left(\frac{\epsilon_r+1}{2}\right)}} \quad (1)$$

$$\epsilon_{eff} = \frac{\epsilon_r+1}{2} + \frac{\epsilon_r-1}{2} \left[1 + 12 \frac{h}{W}\right]^{-1} \quad (2)$$

$$\Delta L = 0.412h \left(\frac{(\epsilon_{eff}+0.3)\left(\frac{W}{h}+0.264\right)}{(\epsilon_{eff}+0.258)\left(\frac{W}{h}+0.8\right)} \right) \quad (3)$$

$$L_g = \frac{0.36 \times c}{f_o \sqrt{\epsilon_{eff}}} \quad (4)$$

$$W_s = \frac{1.38 \times c}{f_o \sqrt{\epsilon_r}} \quad (5)$$

$$L_p = \left(\frac{1}{2f_o \sqrt{\epsilon_{eff}} \sqrt{\mu\epsilon}} - 2\Delta L \right) \quad (6)$$

$$B = \frac{377 \pi}{2 Z_o \sqrt{\epsilon_r}} \quad (7)$$

$$W_f = \frac{2h}{\pi} \left\{ B - 1 - \ln(2B - 1) + \frac{(\epsilon_r - 1)}{2\epsilon_r} \left[\ln(B - 1) + 0.39 - \left(\frac{0.61}{\epsilon_r} \right) \right] \right\} \quad (8)$$

$$L_f = 3.96 \times W_f, \quad (9)$$

where ϵ_{eff} is the effective dielectric constant, h is the height of the dielectric substrate, W_p is the width of the patch, L_{eff} is the effective length of patch, L_p is actual length of patch, ΔL is the length extension, and Z_o is the equivalent feed line impedance. The first and second steps are obtained by trial and error. The dimensions of patch and feed line are demonstrated in Figure 1. The values of the parameters are presented in Table 1.

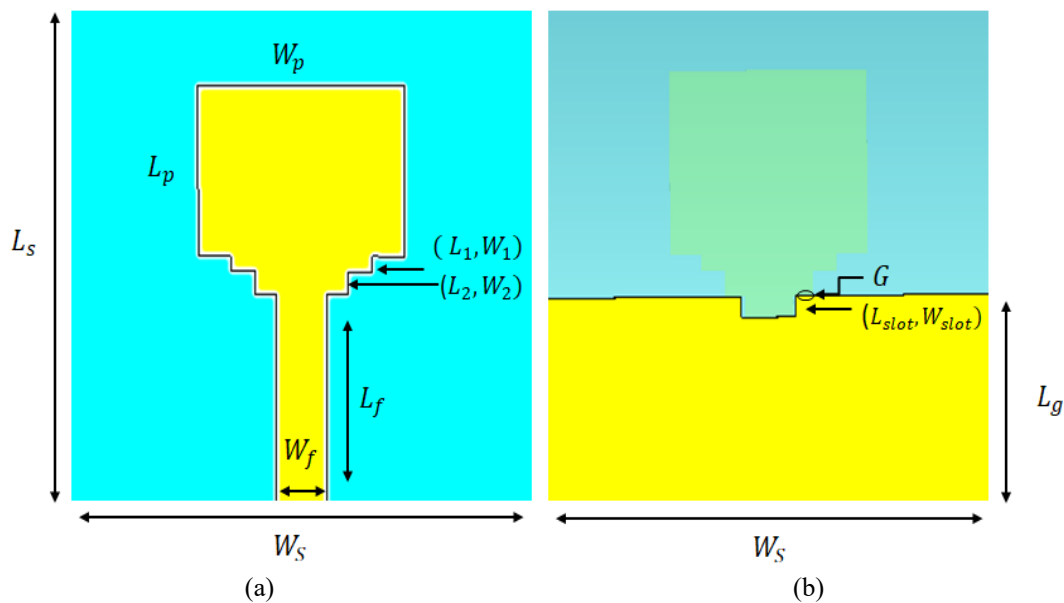


Figure 1. Designs of the UWB MP antenna;
(a) MP antenna and (b) Back view of ground plane

Table 1. Dimensions of the proposed UWB MP antenna

Parameter	Value (mm)	Parameter	Value (mm)
Substrate length, L_s	23.9	First step length, L_1	0.8
Substrate width, W_s	28.5	First step width, W_1	8.7
Ground length, L_g	9.85	Second step length, L_2	1.2
Ground width, W_g	28.5	Second step width, W_2	5.7
Patch length, L_p	8.8	Ground plane slot width, W_{slot}	4.8
Patch width, W_p	12.7	Ground plane slot length, L_{slot}	0.9

The antenna response simulation result for the proposed UWB patch antenna is shown in Figure 2. Figure 2 displays the proposed antenna for a covered bandwidth of 4.27 to 13 GHz and the return loss response has two resonating frequency bands at 5.13 and 9.89 GHz. These frequencies are due to the parameters given in Table 1. The radiation patterns of the resulting antenna are shown in Figure 3. Figure 3 shows the antenna is omnidirectional at frequencies 5.13 and 9.89 GHz with gains of 2.78 and 5 dBi, respectively. With regards to Figure 4, it is obvious that the proposed antenna has acceptable omnidirectional radiation patterns at two specific frequencies.

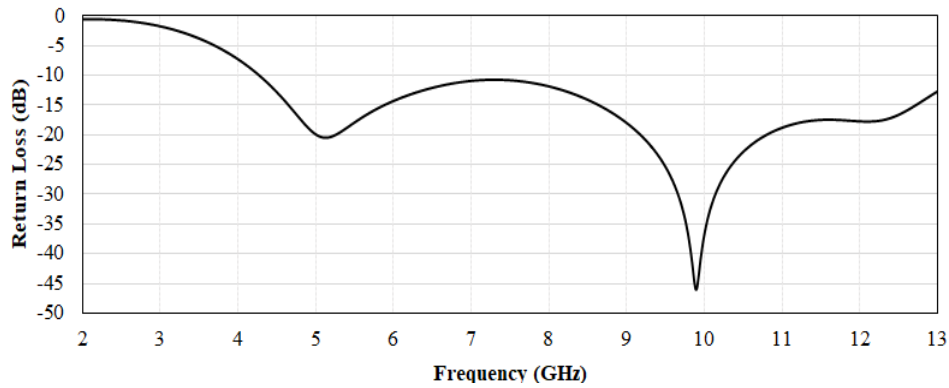


Figure 2. Simulated return loss of the proposed UWB antenna

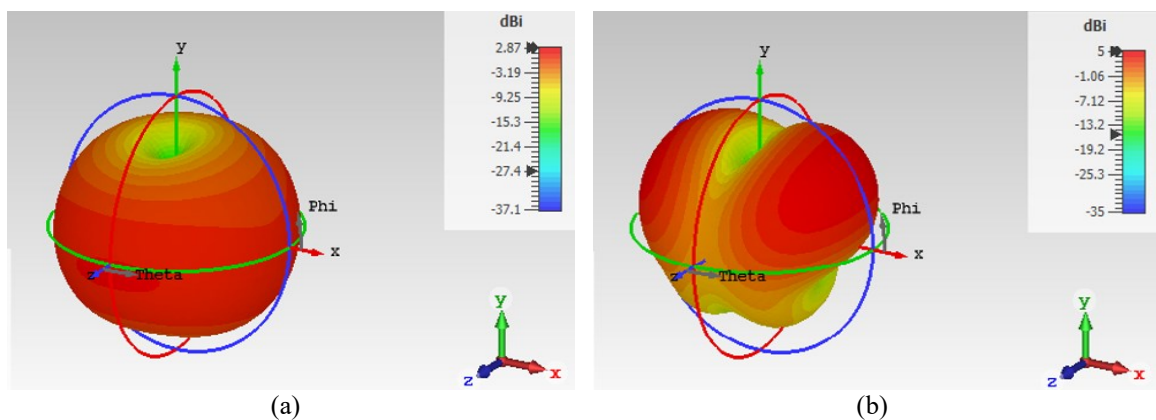


Figure 3. Gain of UWB MP antenna at resonant frequencies; (a) 5.13 GHz and (b) 9.89 GHz

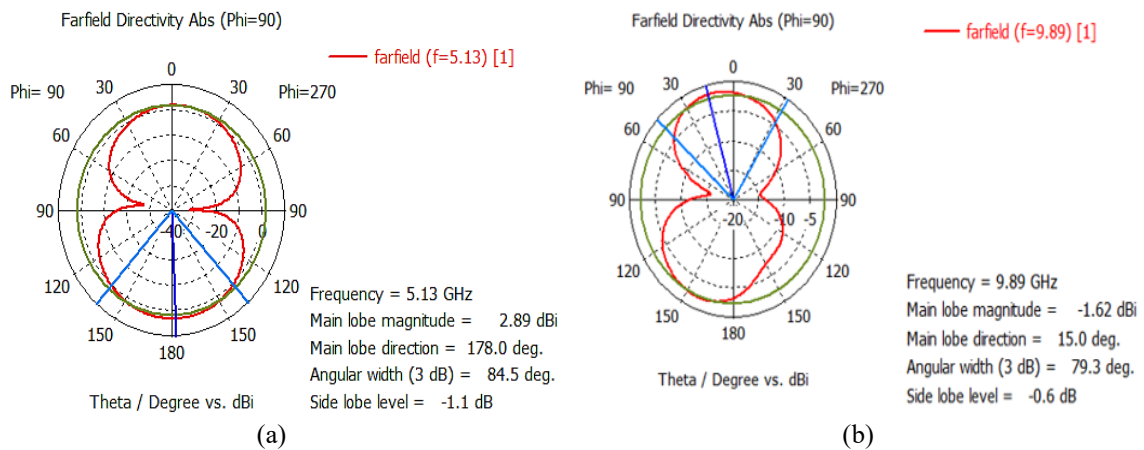


Figure 4. Simulated far-field radiation pattern for the proposed UWB MP antenna design; (a) 5.13 GHz and (b) 9.89 GHz

2.2. Modifications to the UWB MP antenna elements

In order to enhance the antenna’s performance, some modifications needed to be made to obtain notch resonance behaviour. Adjustments were made to the patch, ground plane, feed line, and ground slot the while keeping the essential parameters constant, thus improving the bandwidth. In addition, the patch shape was changed from rectangular to square, to provide a new resonance. Table 2 shows a comparison between the original and modified dimensions. After the modifications, the antenna provides better performance in

terms of bandwidth, gain, and radiation characteristics which can satisfy the requirements of wireless communication applications.

Figure 5 shows the simulated return loss curve of the proposed UWB antenna after modifications. The antenna's performance is quite clear in the operating region from 2.59 to 11.7 GHz, and there are three resonating frequency bands displayed at 3.075 GHz, 5.81 GHz, and 10.54 GHz with return loss of -20.2 dB, -46 dB, and -45.5 dB, respectively. Figure 6 shows the simulated modified gain for each frequency and Figure 7 exhibits the far-field radiation pattern obtained with the enhancement in antenna gain.

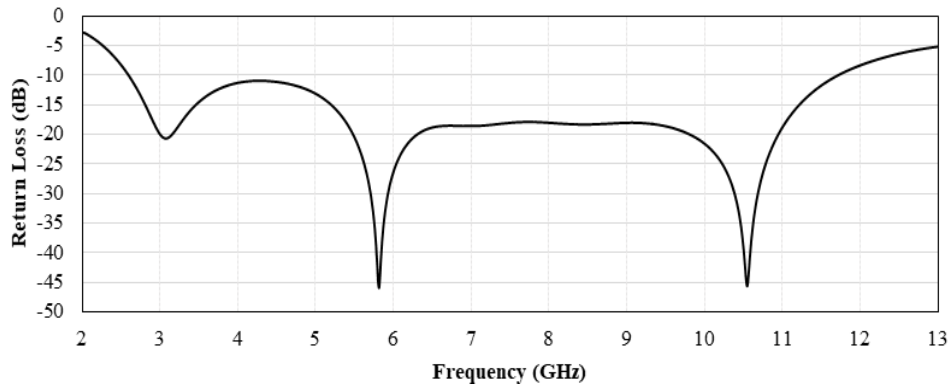


Figure 5. Effects of the modifications on the return loss of the proposed UWB MP antenna

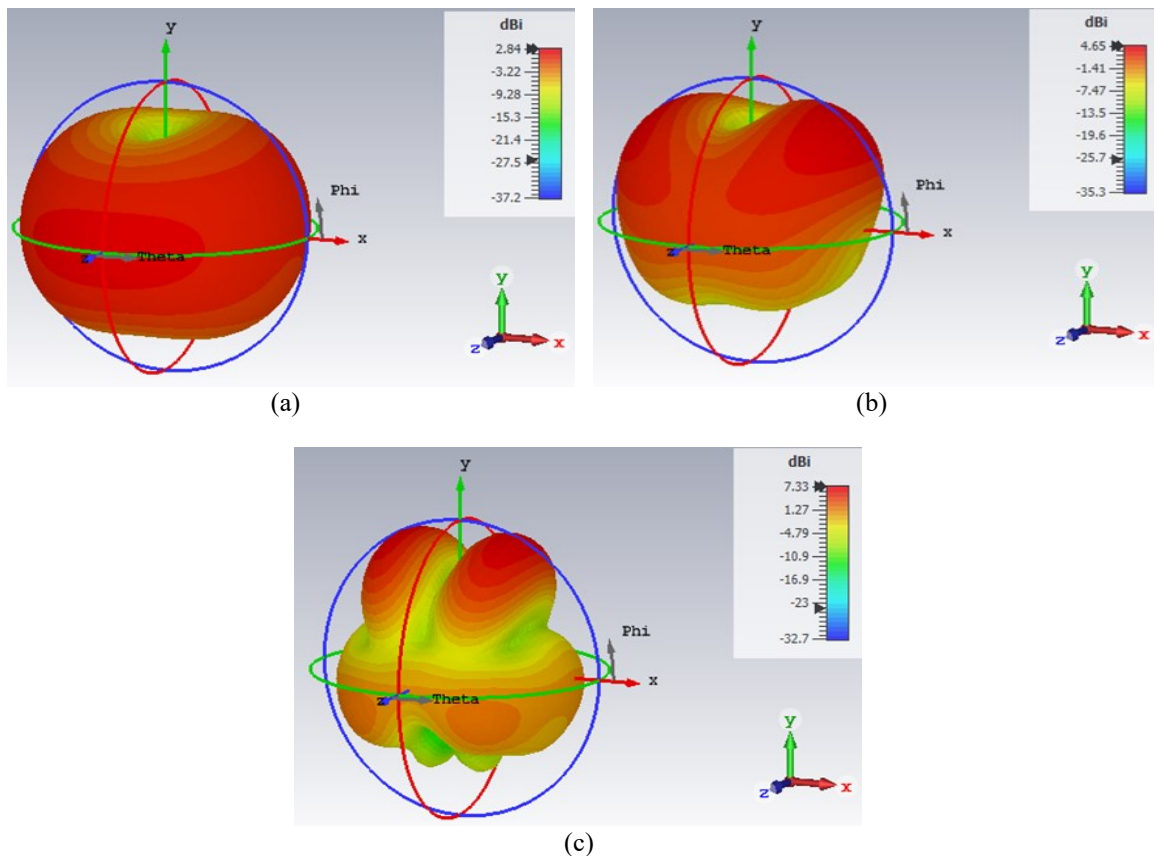


Figure 6. Gains for proposed UWB MP antenna; (a) 3.075 GHz, (b) 5.81 GHz, and (c) 10.54 GHz

Table 2. Comparison between the standard and modified parameters of the UWB MP antenna

Parameter	Calculated Value (mm)	Selected Value (mm)
Substrate length, L_s	23.9	38
Substrate width, W_s	28.5	40
Ground length, L_g	11.8	11.7
Ground width, W_g	28.5	40
Patch length, L_p	8.8	18
Patch width, W_p	12.7	18
Width of the feed, W_f	3.1	3.1
Length of the feed, L_f	9.98	12.2
First step width, W_1	8.7	10.8
Second step width, W_2	5.7	7.6
First step length, L_1	0.8	2.4
Second step length, L_2	1.2	1.2
Gap between patch & ground, G	0.2	0.5
Ground plane slot width, W_{slot}	4.7	3.8
Ground plane slot length, L_{slot}	0.9	2.2

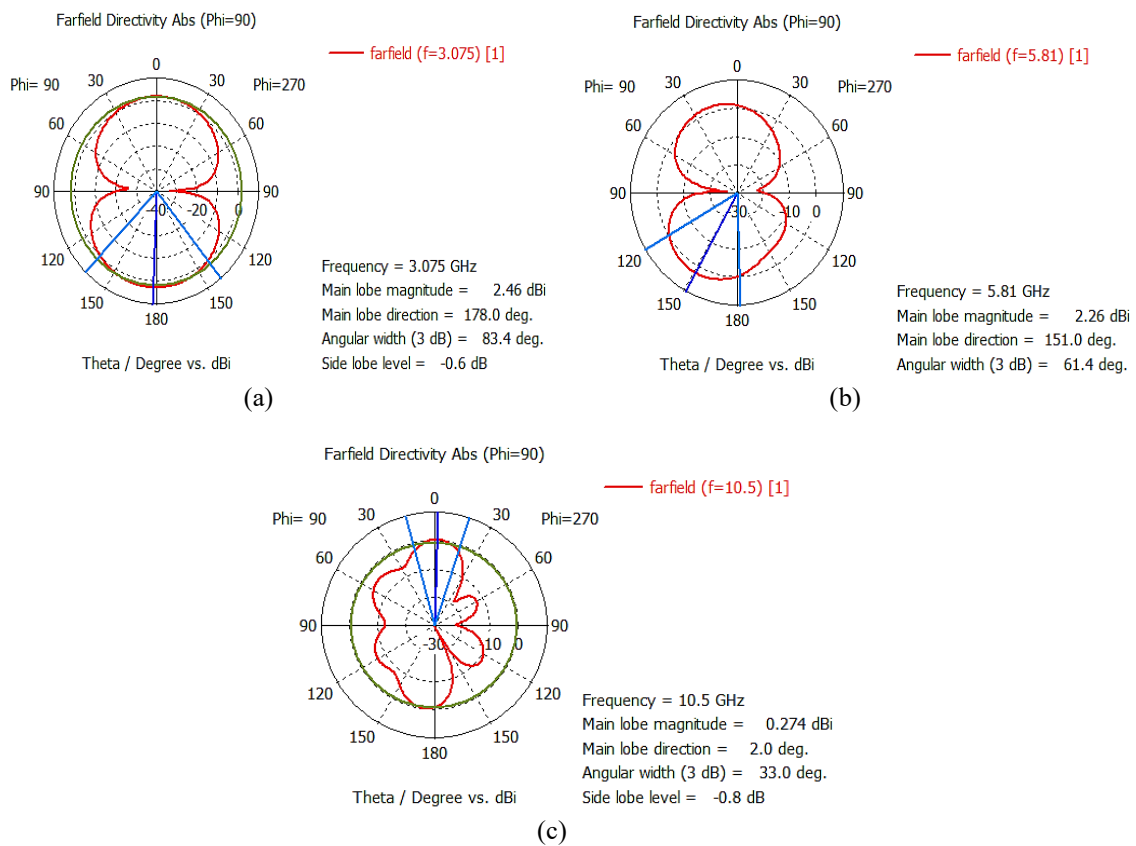


Figure 7. Radiation patterns for proposed UWB MP antenna; (a) 3.075 GHz, (b) 5.81 GHz, and (c) 10.54 GHz

2.3. Implementing the graphene material

Graphene's low weight and thickness (essentially zero), high flexibility, and excellent electronic and electric characteristics distinguish it from other semiconductors. It can be used to obtain a better tuneable frequency and in decreasing or increasing the physical length of the antenna structure [5, 17]. Figure 8 (a) depicts SSG with dimensions ($L_{SSG} \times W_{SSG}$) on the left side of the antenna. Accordingly, there is high current propagation on this side of the antenna and the electric field is concentrated in MP's sides. The physical length of the antenna is affected by the ON and OFF position when the field is applied. Figure 8 (b) represents how the DC voltage can be applied to the graphene material. The chemical potential μ_c (eV) is related to the carrier density n (m^{-2}) as explained in (10):

$$\mu_c \cong \hbar v_f \sqrt{n\pi}, \quad (10)$$

where \hbar or (\hbar -bar) is the reduced Planck's constant ($J\cdot s$) and $v_f=1 \times 10^6$ is the Fermi velocity (m/s) in graphene. Carrier density n is obtained from (11):

$$n = \frac{\varepsilon_0 \varepsilon_r V_b}{dq}, \quad (11)$$

where ε_0 is the vacuum permittivity (F/m), V_b is the DC voltage bias (V), d is the thickness (m), and q is the elementary charge (C). Where the chosen values of V_b , in Table 3, are suitable for devices operating at low voltage.

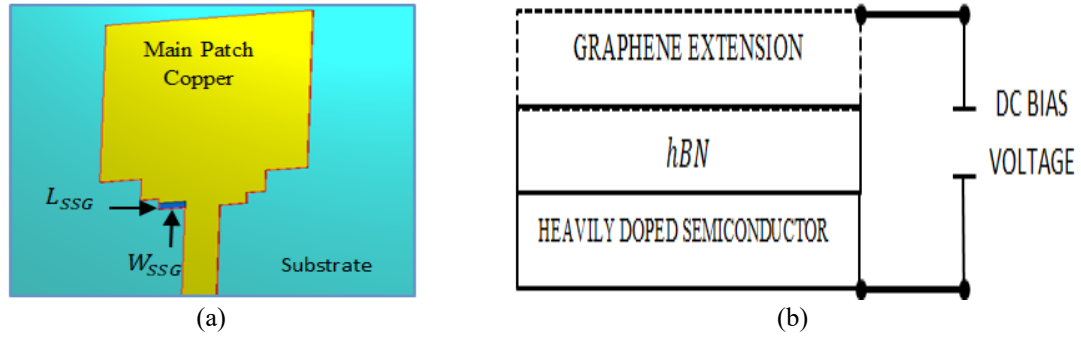


Figure 8. Proposed UWB MP antenna with SSG;
(a) UWB MP antenna and (b) Zoomed view of graphene structure

Table 3. Selected surface impedance Z_s values

Set	1		2	
State	ON	OFF	ON	OFF
$n [m^{-2}]$	2.211×10^{16}	6×10^{14}	1.1×10^{17}	6×10^{14}
$V_b [V]$	1	~ 0	5	~ 0
$\mu_L [m^2/V_s]$	2.7		2.7	
$D [eV]$	4		4	
$T [K]$	295		295	
$Z_s [\Omega / \square]$	$1.05 + j2.3$	$2580 + j6$	$22.35 + j1.03$	$2580 + j6$

In order to obtain functional values of the surface impedances $Z_{s_{ON}}$ and $Z_{s_{OFF}}$ in ON and OFF states, actual values of \mathcal{T}_S and \mathcal{T}_L are required. In addition, a high OFF/ON ratio ($Z_{s_{OFF}}/Z_{s_{ON}}$) is also aimed. The surface resistance values for the ON and OFF states, $Z_{s_{ON}}$ and $Z_{s_{OFF}}$, respectively, provided in Table 3 are calculated from (12):

$$Z_s \approx \frac{j \pi \hbar^2 (2\pi f_0 (\mathcal{T}_L \mathcal{T}_S) - j(\mathcal{T}_L + \mathcal{T}_S))}{q^2 (\mathcal{T}_L \mathcal{T}_S) [\mu_c + 2k_B T \ln(e^{\frac{\mu_c}{k_B T}} + 1)]} \quad (12)$$

where

$$\mathcal{T}_S = \frac{\mu_p \hbar \sqrt{n\mu}}{qv_f} = \frac{4\hbar^2 \rho_m v_{ph}^2 v_f}{\sqrt{n\pi} D^2 k_B T} \quad (13)$$

and

$$\mathcal{T}_L = \frac{\mu_L m^*}{q} \cong \frac{\mu_L \hbar \sqrt{n\pi}}{qv_f}, \quad (14)$$

where \mathcal{T}_S is the short-range scattering [18], \mathcal{T}_L is the long-range scattering [19], k_B is the Boltzmann constant (J/K), T is the temperature (K), μ_L is the electron mobility ($\frac{m^2}{V_s}$), m^* is the carrier mass (Kg) in graphene material, D is the deformation potential (eV), $\rho_m = 7.6 \times 10^{-7}$ is the two dimensional mass density of graphene (Kg/m^2), and $v_{ph} = 2.1 \times 10^4$ is the sound velocity of LA phonons in graphene (m/s) [5, 20].

The Z_{SON} values are obtained via the saturation carrier density n , which is the result of LA phonons scattering and keeping the voltage V_b low (1 V and 5 V). As for Z_{SOFF} , the value is obtained by adjusting the minimum to achieve equal values for the chemical potential and energy of the electron-hole puddles [5]. The carrier inhomogeneity density $\tilde{n} = 6 \times 10^{14} \text{ m}^{-2}$ is obtained from [21], which forces the minimum carrier density n to be greater than or equal to this value $n_{min} \geq \tilde{n}$.

Figure 9 (a) shows the ON state where active voltage DC bias allowing the current to propagate through the graphene sheet. Figure 9 (b) shows the OFF state where the current can't propagate through the graphene sheet and go around it. Consequently, a totally different DC voltage bias ought to be sent through an individual DC bias line to the specified graphene sheet. Table 4 describes some general parameters of such an SSG. It is initially referenced T_{RC} that the time between switching from one operating frequency to another does not need to be quick (on the order of 1 millisecond). The time needed for voltage between the graphene and semiconductor to rise from 50% of the latest value to 90% of that value is known as the switching time [22]. Note that the dielectric thickness d can be decreased by a few nanometres [23]. Finally, the ϵ for the hBN is acquired from [23]. The results were obtained via CST-MWS. The graphene sheet thickness is set to zero and simulated as an ohmic sheet surface resistance based on Table 3.

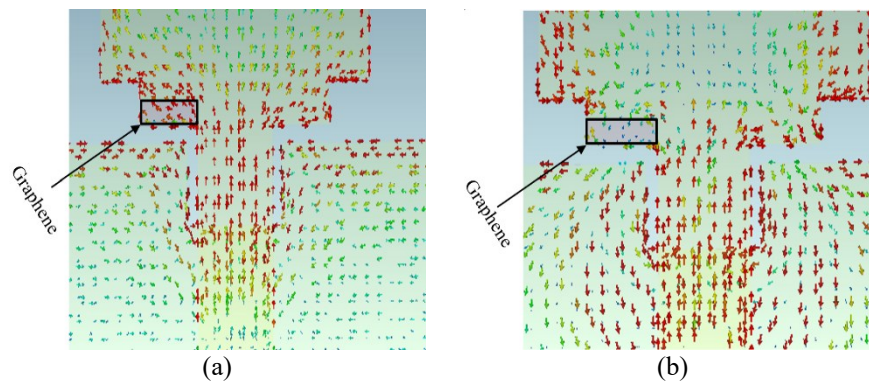


Figure 9. Surface current density in different states; (a) ON state and (b) OFF state

Table 4. Selected general parameters

General Parameters	Value
T_{RC} [ms]	1
Switching time [ms]	1.6
d [nm]	10
ϵ for hBN	4
L_{SSG}	0.7
W_{SSG}	2.3

Figure 10 shows the return loss when the SSG is switched to the ON and OFF states. The new bands that appear cover different microwave applications such as Wi-Fi and Bluetooth vehicular radar systems, which are used to detect the locations and movements of objects near a vehicle, thus enabling features such as near-collision avoidance, improved airbag activation, and suspension systems that are more responsive to road conditions. When the graphene sheet is deactivated (OFF state), the antenna achieved four notch bands at 3.07 GHz, 5.51 GHz, 8.69 GHz, and 11.33 GHz. When the SSG is activated (ON state) at different DC voltage biases based on Table 3: At 1 V, the resonant frequencies changed from 3.07 to 3.05 GHz, 5.51 to 5.59 GHz, and 8.7 to 9 GHz. At 5 V, the resonant frequencies changed from 3.07 to 3.039 GHz, 5.51 to 5.73 GHz, and 8.7 to 10.44 GHz.

The proposed antenna can be utilized for different applications, including S-band (3.07 GHz), which is used for wireless networking (Wi-Fi), airport surveillance radar, and more; C-band (5.51 GHz, 5.73 GHz, and 5.99 GHz), which is used for satellite communications, some wireless devices, and weather radar systems; and X-band (8.7 GHz, 9.01 GHz, 10.44 GHz, and 11.33 GHz) which is used for radar, satellite communication, and wireless networks. These frequency ranges are specified by the IEEE [24, 25]. The activation and deactivation allows the changes between these resonance frequencies without having to make any changes in the antenna's size. Figure 11 shows the UWB MP antenna's gain is reached around 7.33 dBi which it is in acceptable range.

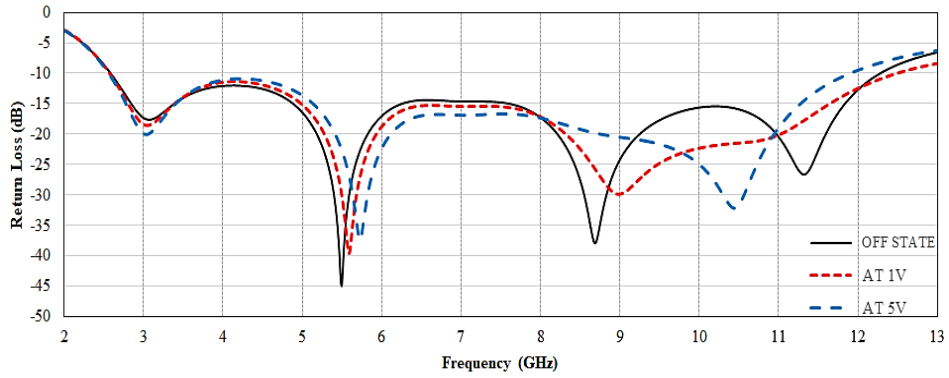


Figure 10. Return loss when the SSG is activated and deactivated

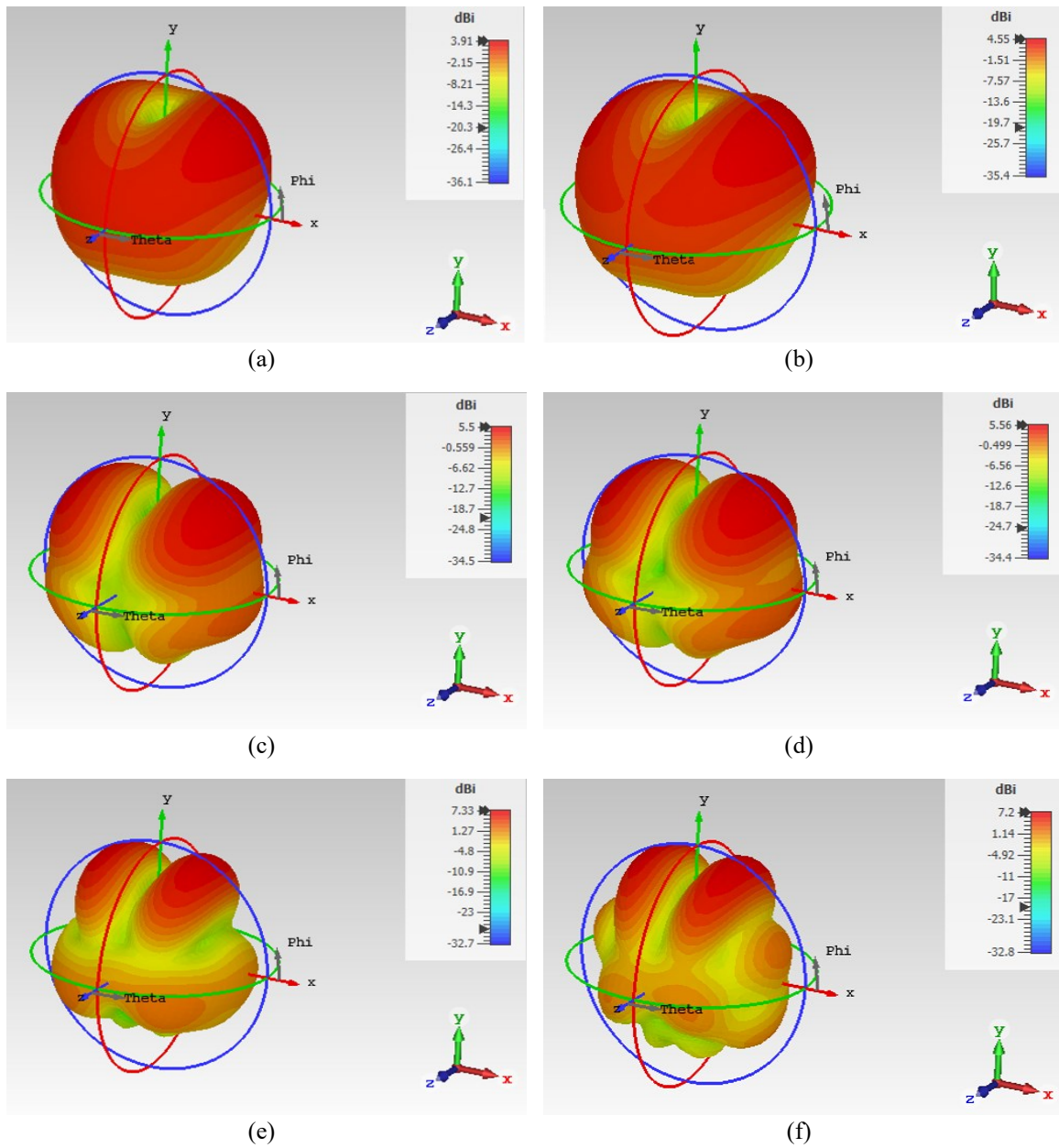


Figure 11. Gains of the UWB MP antenna when the SSG activated and deactivated; (a) 5.51 GHz, (b) 5.73 GHz, (c) 8.69 GHz, (d) 8.98 GHz, (e) 10.44 GHz, and (f) 11.33 GHz

3. RESULTS AND ANALYSIS

The proposed simple MP antenna for UWB applications is illustrated in Figure 1. According to the simulation based on calculated parameters, the return loss under -10 dB was achieved between 4.27 to 13 GHz frequency range. Hence, modifications were made to the design by increasing the dimensions of the antenna and the ground slot dimensions, as shown in Figure 5. The modified antenna operated between 2.59 to 11.7 GHz frequency band and had a new resonance frequency. Thus, it can be used for a new application. The tunable graphene surface's conductivity was maximized by selecting an appropriate place on the antenna based on the surface current and the achieved return loss. Figure 10 showed graphene's effect on the tunable bandwidth of the antenna. When two DC voltage biases (1V and 5V) were applied, the return loss -10 dB was achieved in frequency range between 2.57 to 12.47 GHz and new resonant frequencies were obtained at 5.59 GHz, 5.73 GHz, 8.99 GHz, and 10.44 GHz. The gain values were varied between 2.44 and 7.33 dBi.

4. CONCLUSION

This paper's aim was to enhance the performance of UWB antenna and presented a MP UWB antenna with a ground slot and with good characteristics. Additionally, it had an SSG operating as a tuneable surface in order to minimize the antenna's size and increase its operational bandwidth. Changing the voltage bias applied to the graphene proved to be a good way to enhance the physical size of the antenna while increasing the operational bandwidth. Although the MP antenna had a weak gain characteristic, the proposed design achieved a gain of as much as 7.33 dBi in some frequencies. This design with its UWB feature, small size, and a good performance on the part of the graphene is attractive for; S-band, C-band, and X-band applications.

REFERENCES

- [1] R. Nail and N. Qasem, "Enhancing the Power Spectral Density of PPM-IR for Ultra-Wide Band signals by using a convolutional encoder," *Conferences: 2015 Internet Technologies and Applications (ITA)*, pp. 14-17, 2015.
- [2] N. Qasem and B. Al-Haj Moh'd, "Enhancing the Power Spectral Density of PPM TH-IR UWB Signals Using Sub-Slots Technique," *International Journal of Computer Science and Network Security (IJCSNS)*, vol. 11, no. 1, pp. 341-346, 2017.
- [3] Z. U. Abedin and Z. Ullah, "Design of a Microstrip Patch Antenna with High Bandwidth and High Gain for UWB and Different Wireless Applications," *International Journal of Advanced Computer Science and Applications (IJACSA)*, vol. 8, no. 10, pp. 379-382, 2017.
- [4] Da Yi., et al., "Tunable microwave absorber based on patterned graphene," *IEEE Transactions on Microwave Theory and Techniques*, vol. 65, no. 8, pp. 2819-2826, 2017.
- [5] Christian Nuñez Alvarez, et al., "Performance analysis of hybrid metal-graphene frequency reconfigurable antennas in the microwave regime," *IEEE Transactions on Antennas and Propagation*, vol. 65, no. 4, pp. 1558-1569, 2017.
- [6] A. N. Grigorenko, et al., "Graphene plasmonics," *Nature Photon*, vol. 487, pp. 749-758, 2012.
- [7] S. Sadat, et al., "A compact microstrip square-ring slot antenna for uwb applications," *IEEE Antennas and Propagation Society International Symposium*, vol. 67, pp. 4629-4632, 2006.
- [8] X. S. Rong, et al., "A Graphene Loaded THz Patch Antenna with Tunable Frequency," *In 2018 IEEE World Communication Engineering (WSCE)*, pp. 76-79, 2019.
- [9] D. Yadav and V. Tiwari, "UWB antenna designing: challenges and solutions," *Int'l Journal of Computing, Communications & Instrumentation Engg*, vol. 1, pp. 39-40, 2014.
- [10] Sajid M. Asif, et al., "Design of an ultra-wideband antenna using flexible graphene-based conductor sheets," *IEEE International Symposium on Antennas and Propagation (APSURS)*, pp. 1863-1864, 2016.
- [11] T. Peter, et al., "A novel transparent UWB antenna for photovoltaic solar panel integration and RF energy harvesting," *IEEE Transactions on antennas and propagation*, vol. 62, no. 4, pp. 1844-1853, 2014.
- [12] M. Usman, et al., "Interference Mitigation using Slot cutting in UWB Antenna," *In 2019 2nd International Conference on Computing, Mathematics and Engineering Technologies (iCoMET)*, pp. 1-4, 2019.
- [13] Jianxin Liang, et al., "Study of a printed circular disc monopole antenna for uwb systems," *IEEE transactions on antennas and propagation*, vol. 53, no. 11, pp. 3500-3504, 2005.
- [14] CST MicrowaveStudio. ver. 2019, CST Computer Simulation Technology AG, Darmstadt, Germany, 2019. [Online]. Available: <http://www.cst.com>.
- [15] E. Dheyab and N. Qasem, "Design and optimization of rectangular microstrip patch array antenna using frequency selective surfaces for 60 GHz," *International Journal of Applied Engineering Research*, vol. 11, no. 7, pp. 4679-4687, 2016.
- [16] P. T. Chaudhari, et al., "Printed Circular Monopole Antenna for UWB Applications," *International Journal of Computer Applications*, pp. 11-14, 2014.
- [17] Xing-Shuai Rong, et al., "A Graphene Loaded THz Patch Antenna with Tunable Frequency," *2018 IEEE World Symposium on Communication Engineering (WSCE)*, pp. 76-79, Dec 2019.
- [18] J. H. Chen, et al., "Intrinsic and extrinsic performance limits of graphene devices on SiO₂," *Nat. Nanotechnol.*, vol. 3, pp. 206-209, 2008.

- [19] K. S. Novoselov et al., "Electric field effect in atomically thin carbon films," *Science*, vol. 306, no. 5696, pp. 666-669, 2004.
- [20] E. Carrasco, et al., "Gate-controlled mid-infrared light bending with aperiodic graphene nanoribbons array," *Nanotechnology*, vol. 26, no. 13, pp. 134002, 2015.
- [21] N. Petrone, et al., "Chemical vapor deposition-derived graphene with electrical performance of exfoliated graphene," *Nano Lett.*, vol. 12, no. 6, pp. 2751-2756, 2012.
- [22] R. L. Haupt and M. Lanagan, "Reconfigurable antennas," *IEEE Antennas Propag, Mag*, vol. 55, no. 1, pp. 49-61, 2013.
- [23] K. K. Kim, et al., "Synthesis and characterization of hexagonal boron nitride film as a dielectric layer for graphene devices," *ACS nano*, vol. 6, no. 10, pp. 8583-8590, 2012.
- [24] T. Bhandari and S. Baudha, "An UWB compact microstrip antenna for S band, C band and X band applications," *12th European Conference on Antennas and Propagation (EuCAP 2018)*, pp. 1-5, 2018.
- [25] Khan. I, et al., "A Hepta-band Antenna Loaded with E-shaped Slot for S/C/X-band Applications," *International Journal of Electronics and Telecommunications*, vol 65, no. 2, pp. 167-174, 2019.

BIOGRAPHIES OF AUTHORS



Noor Raheem received his B.Sc. degree in Computer and Communications Engineering from Al-Rafidain University College, Iraq, Baghdad, in 2012. She is studying M.Sc. in Communications Engineering at Al-Ahliyya Amman University, Amman, Jordan.



Nidal Qasem received his B.Sc. degree in Electronics and Communications Engineering (Honours) from Al-Ahliyya Amman University, Amman, Jordan, in 2004. He obtained his M.Sc. degree in Digital Communication Systems for Networks & Mobile Applications (DSC) in 2006, followed by a Ph.D. in Wireless and Digital Communication Systems, both from Loughborough University, Loughborough, United Kingdom. He currently holds the position of associate professor in the department of Electronics and Communications Engineering at Al-Ahliyya Amman University. His research interests include propagation control in buildings, specifically improving the received power, FSS measurements and designs, antennas, ultra-wide band, orbital angular momentum, and wireless system performance analyses. He is a senior member of the IEEE.